Modeling and Analysis of Flexible Bodies Using Lumped Parameter Method

Dipendra Subedi, Ilya Tyapin and Geir Hovland

Department of Engineering Sciences
University of Agder
4879 Grimstad, Norway

Abstract **The modeling, identification and analysis of a flexible beam is presented. The lumped parameter method is used to model a flexible beam. The use of camera measurements to identify lumped parameters, namely spring stiffness and damping coefficient, is described. The measurements of the tip oscillations using a high-speed camera and high-precision laser tracker are compared. The static and dynamic behavior of the flexible beam model is compared to the experimental results to show the validity of the model.**

B.1 Introduction

Development of flexible manipulators is of on-going interest for researchers worldwide. The use of light flexible manipulators has many advantages over conventional industrial robots such as low cost, reduced energy consumption, high payload-to-robot-weight ratio, high operational speed, better transportability, safe operation due to reduced inertia and so on [1]. However, link flexibility causes unwanted oscillations and problems in the precise position control of the end-effector which may even lead to an unstable system. For achieving minimum oscillations and good position accuracy, the industrial robots are designed with highly stiff materials (like heavy steel with bulky design) which consequently require expensive high-power drives.

The vibration of end-effector at high speed and high load is still present due to industrial robot elasticity. In this context, lightweight flexible manipulators are better alternatives if the control architecture is designed to reduce the vibration of the end-effector to an acceptable range. The non-linear dynamics of the system with an infinite number of degrees of freedom make the control of flexible manipulator more complicated than the rigid robots. In order to develop efficient control algorithm for the flexible manipulator, it is necessary to construct a mathematical model of the system incorporating flexibility of the links. Due to impracticability to model the flexible link with infinite degree of freedom for dynamic analysis and simulations, it is necessary to describe the system with finite degree of freedom and still being able

to represent all the dynamically relevant flexibility effects. A dynamically accurate and computationally affordable simulation model is required to represent the actual system behavior to design suitable control algorithm.

The goal of flexible beam modeling is to achieve an accurate model of a flexible manipulator system formed by the combination of multiple flexible links connected together by revolute joints represented by a spring and damper system. This paper represents a part of the work done for modeling a long reach $3R$ planar manipulator constructed using flexible links.

Different models of flexible bodies are available in the literature depending upon the assumptions and required complexity. Accuracy of the models depends on the assumptions made to simplify the complexity of the flexible link manipulator system. There are three main approaches that are used traditionally in the literature: lumped parameter method, assumed mode method and finite element method [2]. In assumed mode method, it is difficult to calculate modes of the link with varying cross-sections [3]. Finite element method is computationally very expensive. Recently, researchers have used lumped parameter method to model flexible arms of multi-link manipulators [4], boom of a mobile concrete pump [5], and other flexible mechanical structures [6].

Lumped parameter method is explored further in this paper because it is a good compromise between the complexity of continuous non-linear dynamical system and the simplicity of neglecting the elasticity with a rigid body model [7]. The computational cost and the accuracy of lumped parameter method can be controlled by changing the number of lumped elements.

Different modeling techniques, control approaches and sensor systems for flexible manipulator are explored in literature [1, 2]. However, there is very limited work done in the experimental identification of model parameters of flexible manipulator. This paper describes a simple approach of identification of lumped parameters of a flexible link using a camera sensor.

In this paper, the lumped parameter method is used to model a flexible beam. High-speed RGB-camera is used to measure the tip oscillations and the high-precision laser tracker to validate the results. The parameters of the flexible beam are identified using camera measurements. The results obtained from the simulation model are compared to the experimental data.

The paper is organized into five sections as follows. The modeling of flexible cantilever beam is described in section B.2. The simulation model is verified with experiments in section B.3. The results obtained from the simulation model are compared to the experimental values in section B.4. Conclusions and discussions follow in section B.5.

B.2 Modeling

The flexible beam is modeled as a set of mass, rotational spring and damper system [2, 7, 8]. The reasons behind using this method for modeling flexibility are simplicity of the method and possibility of extending the model for varying cross-section of the links. Lumped parameter models of a flexible beam with one and two flexible elements are shown in Fig. B.1 and Fig. B.2 respectively. In Fig. B.1, the center of mass is located at the origin of coordinate frame S_1, and k, c, F, M, δ_v, δ_θ represent stiffness, damping coefficient, end load, moment, vertical deflection and angular deflection respectively. In Fig. B.2, two flexible elements are connected in such a way that the spring and damper are in series between two segments. The modeling parameters k and c depend on the dimension and material used in the beam and can be identified/approximated via experiments. The bending of the flexible beam is modeled about one axis, i.e. rotational degree of freedom about the Z-axis.

Considering L, F, E, I as the length of the beam, load attached to the end of the beam,Young's modulus, and area moment of inertia, the vertical tip deflection (δ^u_{vA})

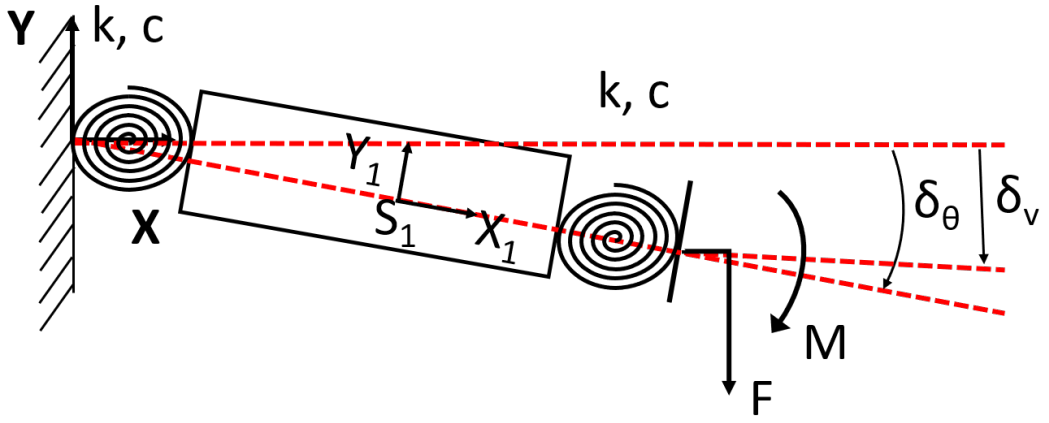

Figure B.1: Lumped parameter model of an end-loaded cantilever flexible beam with one flexible element

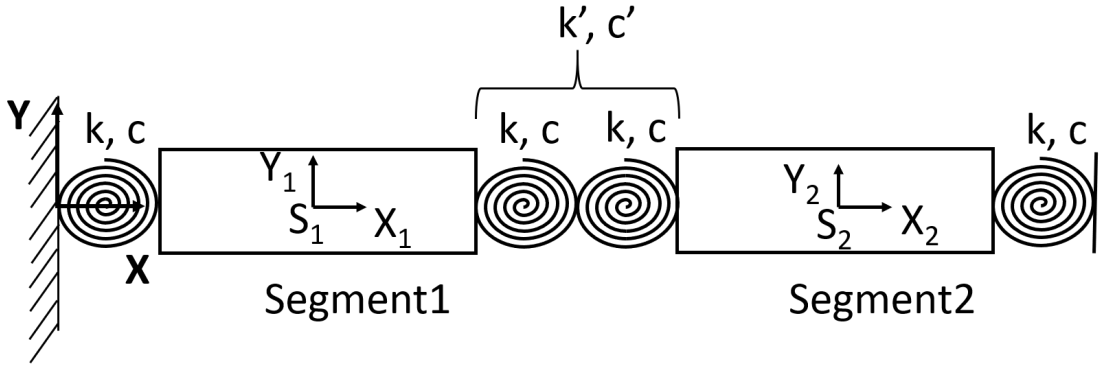

Figure B.2: Lumped parameter model of a flexible beam with two flexible elements

and the angular deflection ($\delta^u_{\theta A}$) of the beam under a uniform load ($q = a\rho g$) is given by (B.1) and (B.2) respectively, where a, ρ, and g are cross-section area, density, and gravity respectively and indices A and u represent analytical solution and uniform load condition respectively [9]. The vertical tip deflection (δ^e_{vA}) of the beam due to end load (F) shown in Fig. B.1 is given by (B.3), where index e represents end load condition. The angular tip deflection ($\delta^e_{\theta A}$) of the cantilever beam due to end load is given by (B.4). The total vertical tip deflection (δ_{vA}) and angular tip deflection ($\delta_{\theta A}$) of the beam are given by a sum of deflection under uniform load and deflection due to end load as given by (B.5).

$$\delta^u_{vA} = \frac{qL^4}{8EI} \tag{B.1}$$

$$\delta^u_{\theta A} = \frac{qL^3}{6EI} \tag{B.2}$$

$$\delta^e_{vA} = \frac{FL^3}{3EI} \tag{B.3}$$

$$\delta^e_{\theta A} = \frac{FL^2}{2EI} \tag{B.4}$$

$$\delta_{\theta A} = \delta^u_{\theta A} + \delta^e_{\theta A}; \quad \delta_{vA} = \delta^u_{vA} + \delta^e_{vA} \tag{B.5}$$

The *equivalent stiffness* of the beam under end-loaded condition is given by (B.6). The *equivalent stiffness* of the beam is used in the lumped parameter model. Both angular and vertical deflections of the beam in lumped parameter model can be approximated using (B.7) and (B.8) respectively, where index L represents lumped parameter approximation.

$$k_A = \frac{FL}{\delta^e_{\theta A}} = \frac{2EI}{L} \tag{B.6}$$

$$\delta^e_{\theta L} = \frac{FL}{k_A} = \frac{FL^2}{2EI} \tag{B.7}$$

$$\delta^e_{vL} = L\delta^e_{\theta_L} = \frac{FL^3}{2EI} \tag{B.8}$$

The angular deflection obtained analytically in (B.4) and using the lumped parameter model in (B.7) are equal. However, the vertical deflection obtained analytically in (B.3) and using the lumped parameter model in (B.8) are not equal.

To improve the approximation in lumped parameter model, the total length of the beam is divided into n_s smaller segments, each segment has a length $L_s = L/n_s$, and the lumped segments are connected together to form the model of the beam.

The stiffness of a single beam segment is given by (B.9). The equivalent stiffness k' of two springs, each of stiffness k, connected in series between two beam segments is given by (B.10). Similarly, the equivalent damping coefficient c' of two dampers c connected in series between two beam segments is given by (B.11) and shown in Fig. B.2.

$$k = \frac{2EI}{L_s} \tag{B.9}$$

$$k' = \frac{k^2}{2k} \tag{B.10}$$

$$c' = \frac{c^2}{2c} \tag{B.11}$$

Considering uniform beam cross-section, the total *equivalent stiffness* (k_{tE}) of the beam can be approximated experimentally, where index E represents experimentally identified value. Using known tip load (F_E), the deflection (δ_{vE}) can be measured to calculate the *equivalent stiffness* by using (B.12). Thus obtained total *equivalent stiffness* of the beam is multiplied by the number of beam segments to obtain individual segment stiffness k_E as given in (B.13).

$$k_{tE} = \frac{F_E L}{\delta^e_{\theta E}} = \frac{2F_E L^2}{3\delta^e_{vE}} \tag{B.12}$$

$$k_E = n_s k_{tE} \tag{B.13}$$

Equations of motion

The model of a flexible beam in Fig. B.3 consists of n_s rigid elements with mass m_i connected together by rotational joints P_i, rotational spring stiffness k_i and damper with damping coefficient c_i, where $i = 1, 2, \ldots, n_s$. The first segment spring stiffness is $k_1 = k$ and damping coefficient is $c_1 = c$. All other segment stiffnesses and dampers are $k_i = k'$ and $c_i = c'$ respectively. The rotation of each element is described by angle φ_i. A Newtonian frame O_I is located at the first rotational joint P_1 of the cantilever beam. Body fixed frame S_i of each element is located at the center of gravity.

Equations of motion are derived using Newton-Euler formulation. Considering J_{Ti} as Jacobian matrix for translational motion, J_{Ri} as Jacobian matrix for rotational motion, p_i as linear momentum, l_i as angular momentum, F_i as applied forces, M_i as applied moments for body i, the principles of linear and angular momentum are

applied to get (B.14).

$$\sum_{i=1}^{n_s}[J_{Ti}^T(\dot{p}_i - F_i) + J_{Ri}^T(\dot{l}_i - M_i)] = 0 \tag{B.14}$$

Considering r_{s_i} as the position vector from Newtonian frame O_I to body fixed frame S_i, r_{p_i} as the position vector from Newtonian frame O_I to joint P_i, R_i as the rotation matrix representing rotation of frame S_i with respect to frame O_I about the Z axis, I_i as the inertia tensor, v_{s_i} as the linear velocity, ω_i as the angular velocity, and calculating the translational parts in frame O_I and rotational parts in body reference frame S_i, (B.14) can be written to (B.16) using (B.15) where the cross product $\omega \times r$ is replaced by matrix operation $\tilde{\omega}r$. The mass of tip load is added to m_{n_s} for the last segment.

$$\dot{p}_i = m_i\ddot{r}_{s_i}; \quad \dot{l}_i = I_i\dot{\omega}_i + \tilde{\omega}_i I_i\omega_i \tag{B.15}$$

$$\sum_{i=1}^{n_s} J_{Ti}^T[m_i\ddot{r}_{s_i} - F_i] + J_{Ri}^T[I_i\dot{\omega}_i + \tilde{\omega}_i I_i\omega_i - M_i] = 0 \tag{B.16}$$

Kinematics of the bodies in generalized coordinates $q = (\varphi_1, \varphi_2, \cdots, \varphi_{n_s})^T$ is given by (B.17).

$$\left.\begin{aligned}
R_i &= \begin{bmatrix} cos\varphi_i & -sin\varphi_i & 0 \\ sin\varphi_i & cos\varphi_i & 0 \\ 0 & 0 & 1 \end{bmatrix} \\
r_{p_i} &= r_{p_{i-1}} + R_{i-1}[L_s; 0; 0], \quad r_{p_1} = [0; 0; 0] \\
r_{s_i} &= r_{p_i} + R_i[L_s/2; 0; 0] \\
J_{Ti} &= \frac{\partial r_{s_i}}{\partial q} \\
v_{s_i} &= J_{Ti}\dot{q} \\
\omega_i &= [0; 0; \dot{\varphi}_i] \\
J_{Ri} &= \frac{\partial \omega_i}{\partial \dot{q}} \\
\ddot{r}_{s_i} &= J_{Ti}\ddot{q} + \frac{\partial v_{s_i}}{\partial q}\dot{q} \\
\dot{\omega}_i &= J_{Ri}\ddot{q} + \frac{\partial \omega_i}{\partial q}\dot{q}
\end{aligned}\right\} \tag{B.17}$$

Using the kinematic equations, (B.16) can be rearranged to (B.18). The applied forces are given by the weight of the beam segments and the applied moments by the rotational springs and dampers. In addition, the applied force and moment by

the end-load is considered for the last segment of the beam.

$$\sum_{i=1}^{n_s} \left\{ -J_{Ti}^T [m_i \frac{\partial v_i}{\partial q} \dot{q} - F_i] - J_{Ri}^T [I_i \frac{\partial \omega_i}{\partial q} \dot{q} + \tilde{\omega}_i I_i \omega_i - M_i] \right\} - \\ - \sum_{i=1}^{n_s} \left\{ m_i J_{Ti}^T J_{Ti} + J_{Ri}^T I_i J_{Ri} \right\} \ddot{q} = 0 \tag{B.18}$$

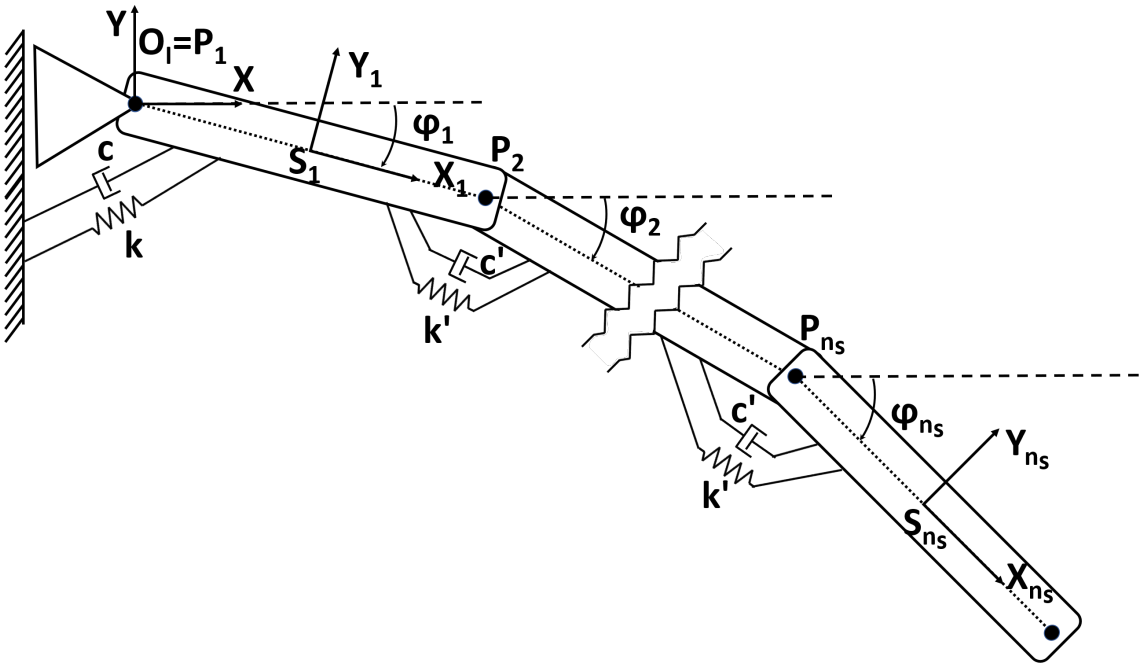

Figure B.3: Model of a flexible beam with n_s dofs

B.3 Simulations and Experiments

A hollow rectangular aluminium beam of length $L = 2.32\ m$, width $W = 0.04\ m$, height $H = 0.04\ m$, thickness $T = 2 \times 10^{-3}\ m$, density $\rho = 2700\ kg/m^3$, Young's modulus $E = 69 \times 10^9\ Pa$ is used in the simulation and experimental studies. The area moment of inertia I of the hollow rectangular beam is calculated using (B.19).

$$I = \frac{1}{12} W H^3 - \frac{1}{12} (W - 2T)(H - 2T)^3 \tag{B.19}$$

A load of $m_l = 4.5\ kg$ is applied at the tip of the beam and the corresponding deflection at the tip is recorded in the simulation and compared to the experimental data. The analytical vertical tip deflection obtained from (B.3) is $\delta_{vA}^e = 0.0363\ m$.

B.3.1 Simulation of analytical lumped parameter model

The stiffness of each flexible element/segment of the beam is calculated using (B.9) and (B.10). The deflection of the tip of the beam due to uniform load (δ^u_{vL}), end-load (δ^e_{vL}) and total deflection (δ_{vL}) for different values of n_s is shown in table B.1 (using *MATLAB ode23* for time integration with fixed step size of 0.01 s).

Dynamic response

To show the dynamic response of the tip of the beam, tip load of 4.5 kg is dropped after ensuring that the tip is stationary before dropping. To reduce the frequency of vibration a body ($m_d = 2.5\ kg$) is mounted at the tip. Moreover, the weight of the camera mounted at the tip is also considered in the simulation. The damping coefficient $c = \beta k$ is used in the simulation, where $\beta = 2.2 \times 10^{-4}$ is the tuning factor. To simulate the oscillation produced only due to the drop, the initial tuning factor is increased 5 times to ensure quick damping (before dropping). The position of the tip of the beam is shown in Fig. B.4. The frequency of vibration of the model ($n_s = 10$) is $f = 3.42\ Hz$.

B.3.2 Experimental identification of stiffness and damping ratio

A 7×9 checkerboard is mounted on the wall in such a way that it is completely visible from the camera when the beam is oscillating. The camera is calibrated intrinsically before mounting on the beam. The position of the checkerboard with

Table B.1: Tip deflection taking different number of flexible elements using analytically obtained lumped parameters

$\mathbf{n_s}$	$\delta^{\mathbf{u}}_{\mathbf{vL}}(\mathbf{m})$ $(m_l = 0kg)$	$\delta_{\mathbf{vL}}(\mathbf{m})$ $(m_l = 4.5kg)$	$\delta^{\mathbf{e}}_{\mathbf{vL}} = \delta_{\mathbf{vL}}$ - $\delta^{\mathbf{u}}_{\mathbf{vL}}(\mathbf{m})$
1	0.0115	0.0387	0.0272
2	0.0072	0.0480	0.0408
3	0.0064	0.0447	0.0383
4	0.0060	0.0435	0.0375
5	0.0060	0.0430	0.0370
6	0.0059	0.0427	0.0368
7	0.0059	0.0425	0.0366
8	0.0059	0.0424	0.0365
9	0.0058	0.0424	0.0366
10	0.0058	0.0423	0.0365

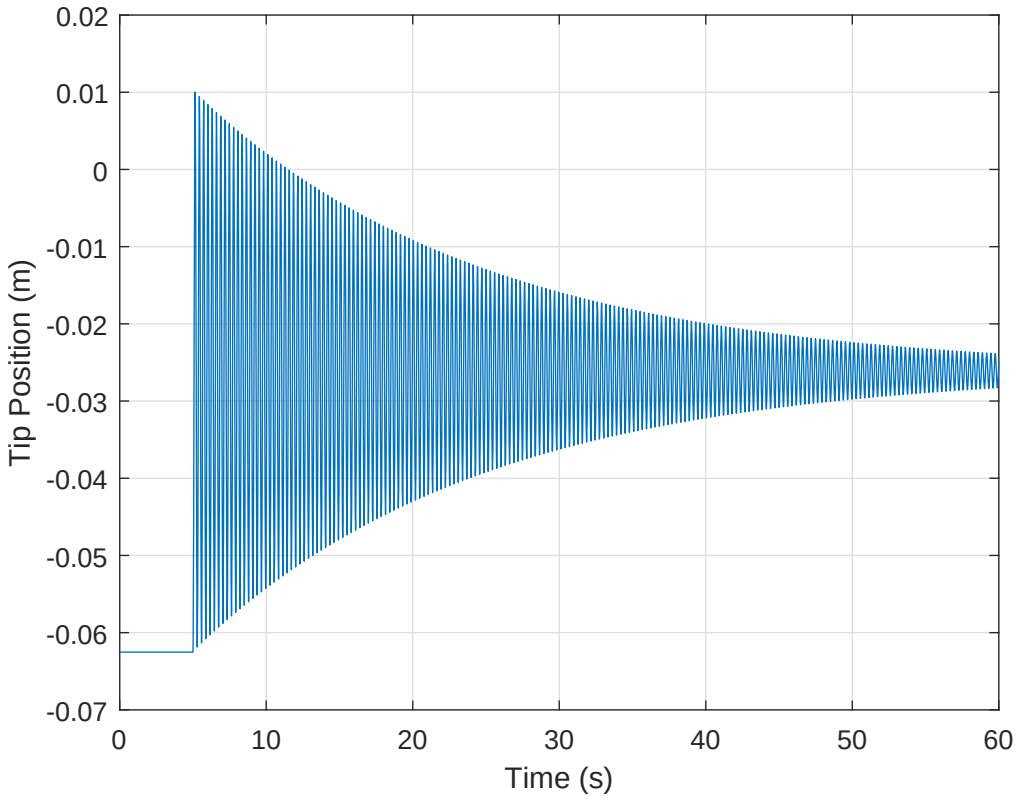

Figure B.4: Tip oscillations using analytical parameters

respect to a camera is determined using *OpenCV*.

In Fig. B.5, an experimental setup consisting of flexible beam (2) mounted on the wall (1) is shown. A spherically mounted retroreflector (3) is mounted at the tip of the beam to track the position of the tip using Leica AT960 laser tracker. Basler ace (acA2040-180kc) color camera (4) is mounted at the tip of the wall mounted cantilever beam and is connected to the computer via a connector (7). Object (6) to be dropped is hanging in the rope (8) at the tip of the beam. Additional object (5) is mounted at the tip to reduce the frequency of oscillation. The initial tip position of the beam is recorded before applying any load at the tip. Then a load of $m_l = 4.5\ kg$ is applied to the tip of the beam and the corresponding deflection of the tip is recorded. The difference gives the deflection (δ^e_{vE}) caused due to the load at the tip. Using (B.12), the total *equivalent stiffness* k_{tE} of the beam is determined. From (B.10) and (B.13), the stiffnesses (k_{1E} and k_{2E}) of each flexible element of the beam are approximated for n_s segments. Experimentally approximated parameters are $\delta^e_{vE} = 0.0403\ m$ and $k_{tE} = 3.8991 \times 10^3\ Nm/rad$.

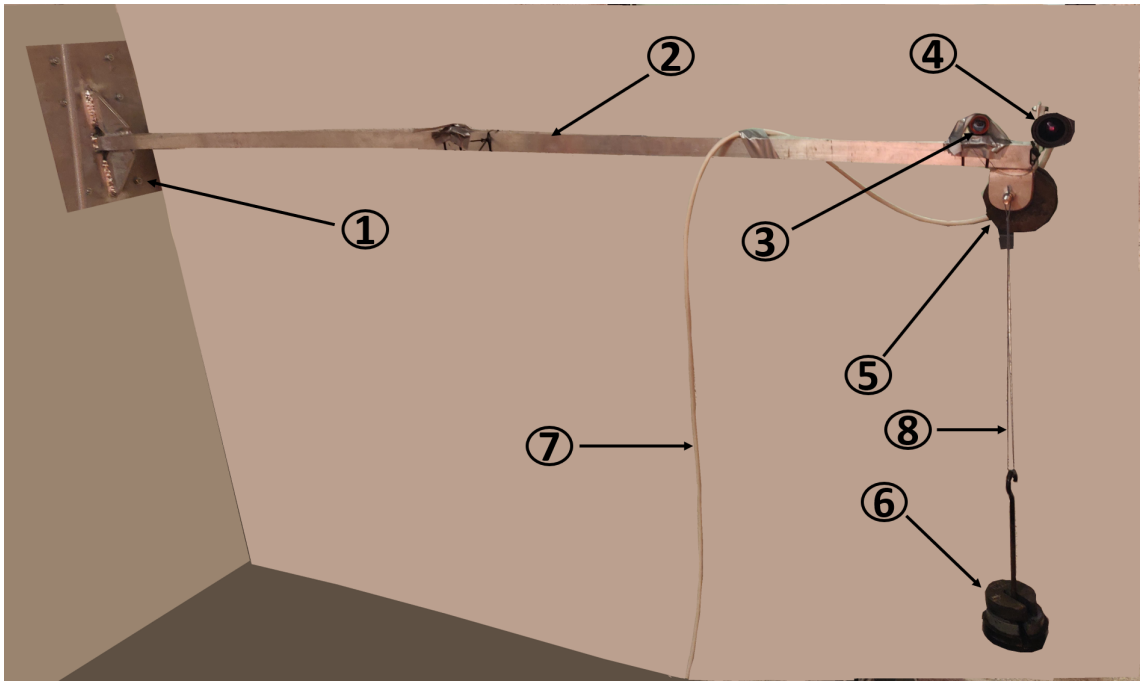

Figure B.5: Experimental setup (1. Wall mount, 2. Flexible beam, 3. Leica spherically mounted retroreflector ball probe, 4. Camera, 5. Tip load, 6. Tip load to be dropped, 7. Camera connector,8. Rope)

Dynamic response

The position of the tip of the beam recorded experimentally using camera is shown in Fig. B.6. The frequency of vibration (eigen frequency) of the beam is $f_E = 3.24\ Hz$. The damping ratio ζ is approximated by calculating logarithmic decrement δ using (B.20) and (B.21) where A_1 and A_n are two successive amplitudes n periods apart [10].

$$\delta = \frac{1}{n} ln \frac{A_1}{A_n} \tag{B.20}$$

$$\zeta = \frac{1}{\sqrt{1 + (2\pi/\delta)^2}} \tag{B.21}$$

The damping coefficient c_{te} is approximated using (B.22) where $\omega_d = 2\pi f_E$ is the frequency of vibration.

$$c_{tE} = 2\zeta\omega_d \tag{B.22}$$

For simulation purposes, the damping coefficient c_E for each flexible element of the flexible beam is approximated using (B.23) where β is the tuning parameter to match simulation model with the experiment. Experimentally approximated parameters are $c_{tE} = 0.08\ Nms/rad$, $\beta = 12$.

$$c_E = \beta n_s c_{tE} \tag{B.23}$$

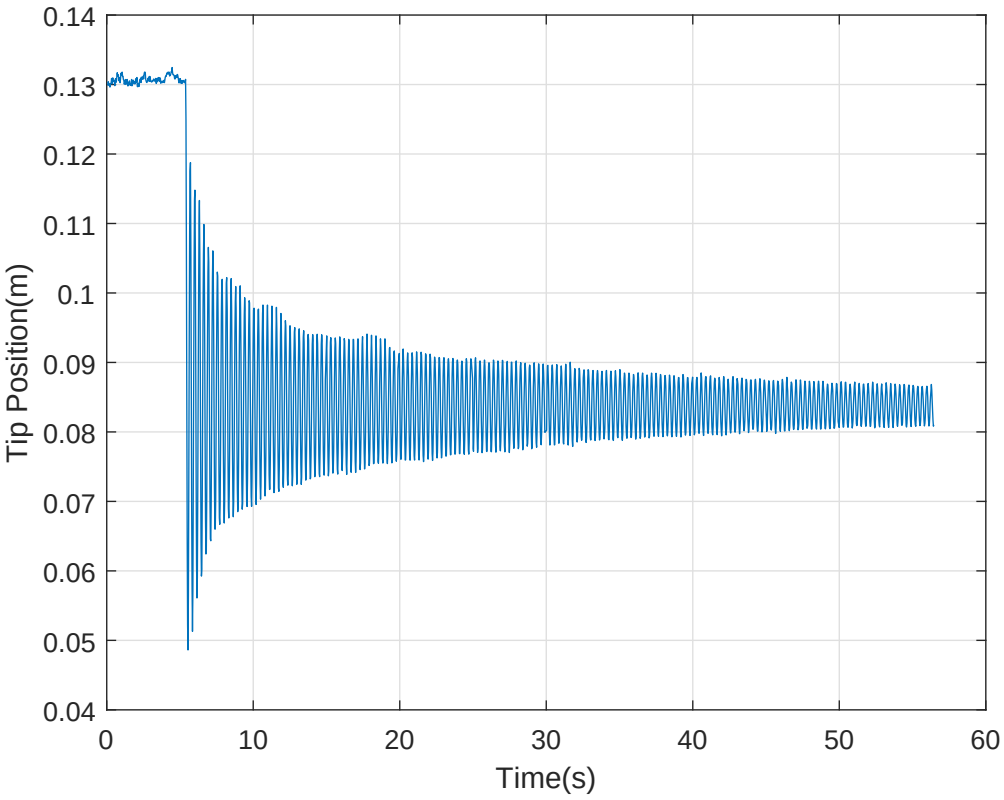

Figure B.6: Tip oscillations recorded using camera

B.3.3 Simulation of experimentally identified lumped parameter model

The stiffness of each flexible elements/segments of the beam approximated experimentally is used in the lumped model of the beam and the corresponding deflection of the tip due to uniform load (δ^u_{vL}), end-load (δ^e_{vL}) and total deflection (δ_{vL}) for different values of n_s is shown in table B.2 (using *MATLAB ode23* for time integration with fixed step size of 0.01 s).

Dynamic response

The position of the tip of the beam using experimentally identified parameters in the model($n_s = 10$) is shown in Fig. B.7. To ensure quick damping in the beginning (before dropping), the tuning parameter β is increased by 5 times. The frequency of vibration of the beam is $f_{Em} = 3.24\ Hz$.

Table B.2: Tip deflection taking different number of flexible elements using experimentally identified lumped parameters

$\mathbf{n_s}$	$\delta^{\mathbf{u}}_{\mathbf{vL}}(\mathbf{m})$ $(m_l = 0kg)$	$\delta_{\mathbf{vL}}(\mathbf{m})$ $(m_l = 4.5kg)$	$\delta^{\mathbf{e}}_{\mathbf{vL}} = \delta_{\mathbf{vL}}$ - $\delta^{\mathbf{u}}_{\mathbf{vL}}(\mathbf{m})$
1	0.0129	0.0434	0.0305
2	0.0081	0.0537	0.0456
3	0.0072	0.0500	0.0428
4	0.0068	0.0487	0.0419
5	0.0067	0.0481	0.0414
6	0.0066	0.0478	0.0412
7	0.0066	0.0477	0411
8	0.0065	0.0475	0.0410
9	0.0065	0.0475	0.0410
10	0.0065	0.0474	0.0409

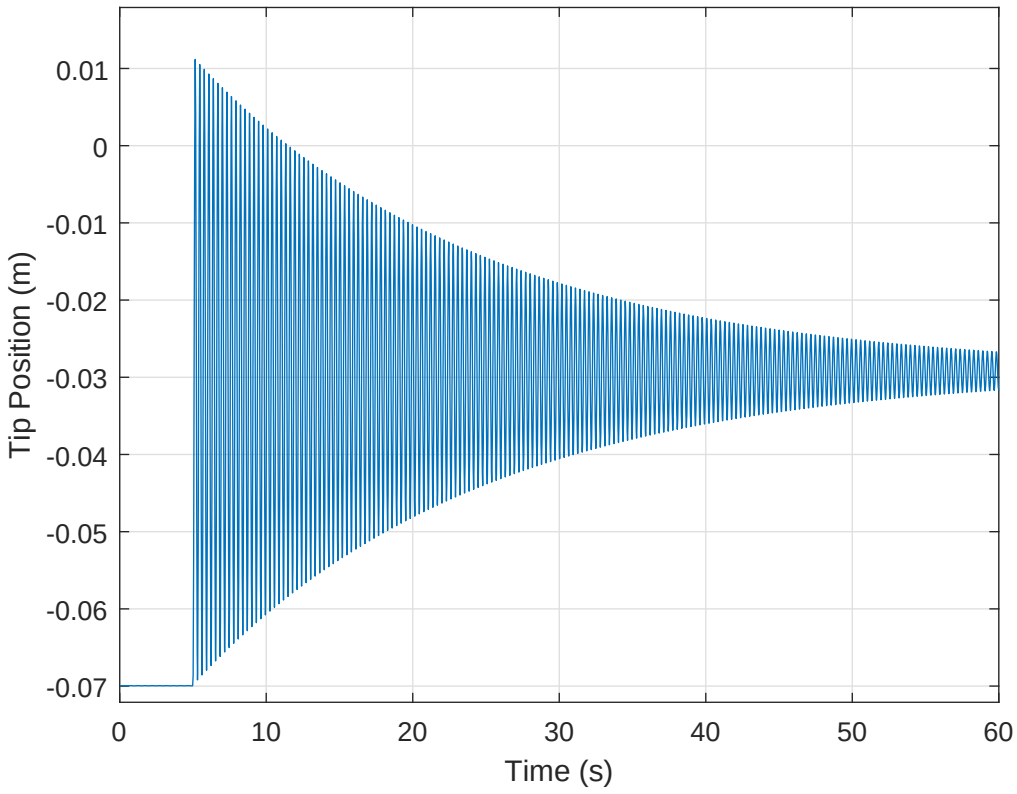

Figure B.7: Tip oscillations using experimentally identified parameters

B.4 Results

The position of the tip of the beam recorded by a camera and laser tracker is shown in Fig. B.8. The possibility of using camera for detecting the oscillations in a flexible structure seems promising. The static deflection due to 6.5 kg load at the end obtained from the experiments using a camera and static deflection approximated from the model ($n_s = 10$) are 0.0583 m and 0.0590 m respectively. Analytically computed static deflection due to 6.5 kg end load from (B.3) is 0.0524 m which is less accurate than the one approximated from the simulation model. It can be seen that the simulation model, where experimentally identified parameters are used, is accurate enough to approximate the static deflection of the real system.

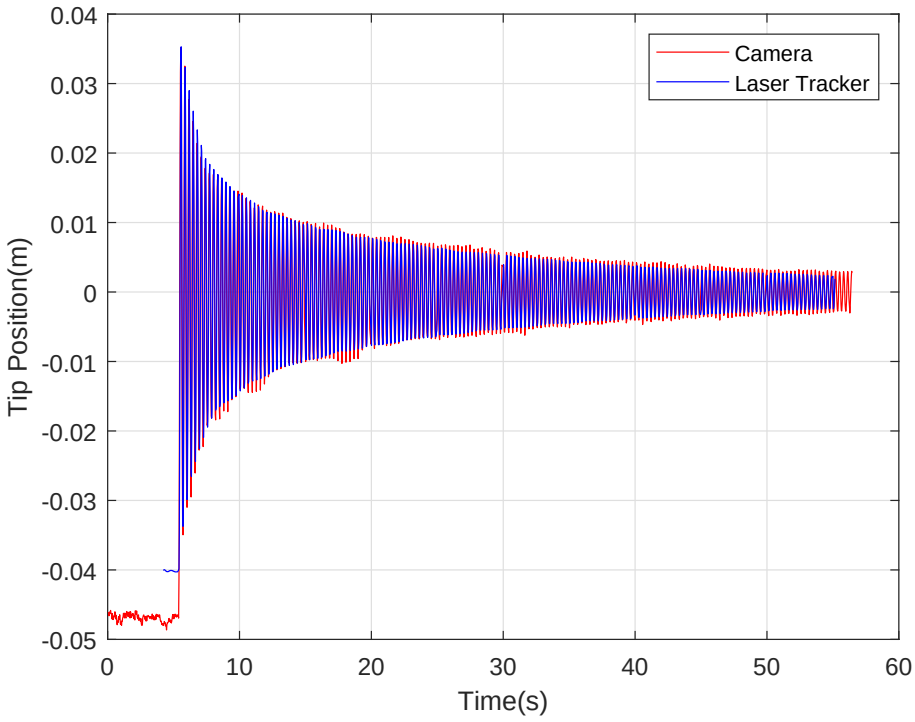

Figure B.8: Tip oscillations using camera and laser tracker

To show the validity of the model, damping load $m_d = 4.5\ kg$ is mounted at the end including the mass of the camera and the end load of $m_l = 4.5\ kg$ is dropped. The corresponding oscillations of the tip recorded by a camera are shown in Fig. B.9. The frequency of the beam vibration obtained from the experimental data collected by a camera is $f_{Ev} = 2.42\ Hz$. The oscillations of the tip obtained from the simulation model ($n_s = 10$) are shown in Fig. B.10. The frequency of vibration of the beam obtained from the simulation model is $f_{mv} = 2.51\ Hz$. The error in frequency of oscillation in the model is approximately 5 %.The tuning parameter β used in simulations is 12.

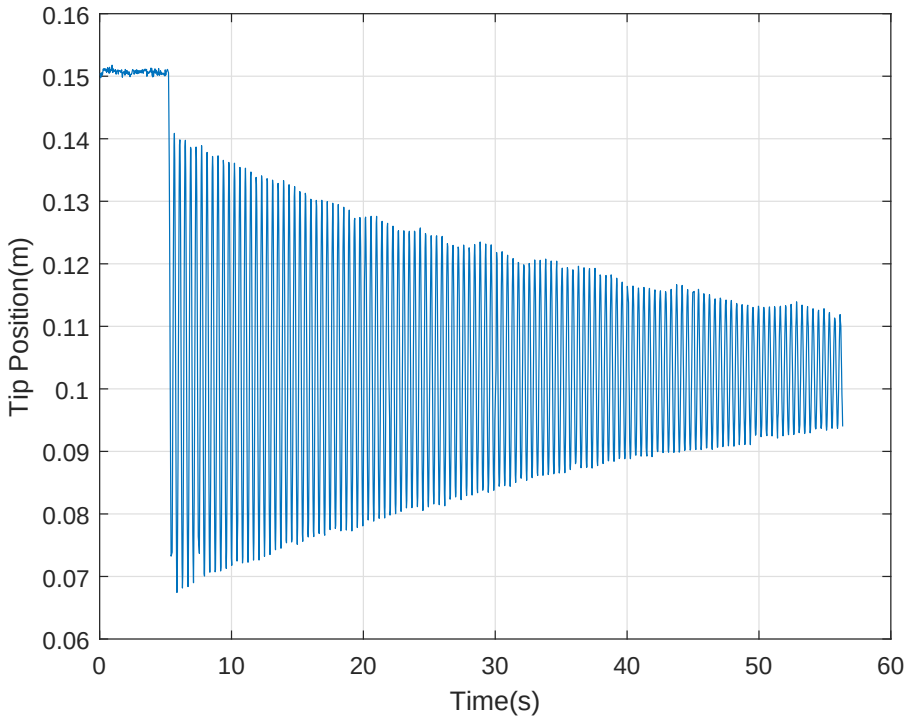

Figure B.9: Tip oscillations recorded using camera for validation

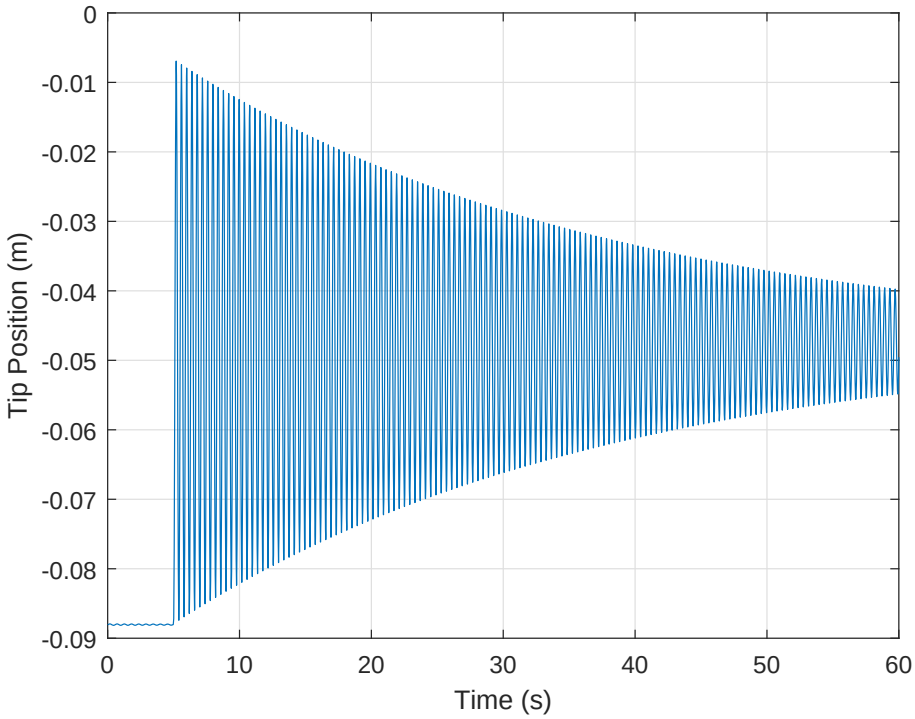

Figure B.10: Tip oscillations using experimentally identified parameters for validation

B.5 Conclusions and Discussions

The accuracy of the static deflection and computational cost increase with the increase in the number of flexible segments. A simulation model of flexible cantilever beam is developed using lumped parameter method. The static and dynamic behavior of the model are compared with the experimental results. The use of camera to identify the lumped parameters of a flexible structure experimentally is presented. The proposed method can be used to model a beam of composite/custom material whose modulus of elasticity is unknown. Although the experimental identification of the lumped parameters gives better approximation of the actual system, the analytically determined parameters could be used with reduced accuracy whenever the experiments are not feasible.

In the next step of the project, the work will be extended to the modeling of flexible beam with varying cross-section and to the development of simulation model for multi-link flexible manipulator. Furthermore, development of a procedure to tune β and ways of reducing error in the oscillation frequency will be explored.

Acknowledgment

The work was funded by the Norwegian Research Council, project number 261647/O20. The authors thank lab engineers at the University of Agder for helping to build the experimental setup.

References – Paper B

[1] Chang Tai Kiang, Andrew Spowage, and Chan Kuan Yoong. Review of control and sensor system of flexible manipulator. *Journal of Intelligent & Robotic Systems*, 77(1):187–213, 2015.

[2] Santosha Kumar Dwivedy and Peter Eberhard. Dynamic analysis of flexible manipulators, a literature review. *Mechanism and machine theory*, 41(7): 749–777, 2006.

[3] Rex J Theodore and Ashitava Ghosal. Comparison of the assumed modes and finite element models for flexible multilink manipulators. *The International journal of robotics research*, 14(2):91–111, 1995.

[4] Ivan Giorgio and Dionisio Del Vescovo. Non-linear lumped-parameter modeling of planar multi-link manipulators with highly flexible arms. *Robotics*, 7(4):60, 2018.

[5] Julian Wanner and Oliver Sawodny. A lumped parameter model of the boom of a mobile concrete pump. In *2019 18th European Control Conference (ECC)*, pages 2808–2813. IEEE, 2019.

[6] Carmine Maria Pappalardo and Domenico Guida. Development of a new inertial-based vibration absorber for the active vibration control of flexible structures. *Engineering Letters*, 26(3), 2018.

[7] Wisama Khalil and Maxime Gautier. Modeling of mechanical systems with lumped elasticity. In *Proceedings 2000 ICRA. Millennium Conference. IEEE International Conference on Robotics and Automation. Symposia Proceedings (Cat. No. 00CH37065)*, volume 4, pages 3964–3969. IEEE, 2000.

[8] G Zhu, Shuzhi Sam Ge, and Tong Heng Lee. Simulation studies of tip tracking control of a single-link flexible robot based on a lumped model. *Robotica*, 17 (1):71–78, 1999.

[9] Dr James Gere and Barry J Goodno. *Mechanics of Materials, SI Edition*. Cengage Learning, 2017.

[10] Daniel J Inman and Ramesh Chandra Singh. *Engineering vibration*, volume 3. Prentice Hall Englewood Cliffs, NJ, 1994.